ARCHIVES OF ACOUSTICS
5, 4, 315-336 (1980)

EXPERIMENTAL DETERMINATION AND PRACTICAL APPLICATION OF THE FOUR-POLE PARAMETERS OF STRUCTURE-BORNE SOUND ISOLATORS

G. MELTZER, R. MELZIG-THIEL

Zentralinstitut für Arbeitschutz DDR (8020 Dresden, Gerhart-Hauptmann-Strasse)

Theoretical fundamentals are derived for measuring the four-pole parameters of vibration isolators at real loads. Since the dynamic properties of rubber springs depend on the initial load, the vibration force and velocity are measured on the isolator interfaces for a given initial load. Four-pole parameters are determined for rubber springs and steel springs. The frequency characteristics of the parameters, calculated from the measured results, are compared with the theoretical frequency characteristics. Furthermore, approximate relations for the determination of the four-pole parameters are derived, and verified by experiments. Practical application of the four-pole parameters of vibration isolators is illustrated by examples in which calculations are performed for: structure-borne sound wave isolation by longitudinally vibrating continua and the excitation of structure-borne sound by machines.

Nomenclature*

A — cross-sectional area
$\mathfrak{A}_{11}, \mathfrak{A}_{12}, \mathfrak{A}_{21}, \mathfrak{A}_{22}$ — complex four-pole parameters,
E — elastic modulus,
$\mathfrak{F}$ — complex force,
$\mathfrak{F}_0$ — short-circuit force,
$\mathfrak{F}_1, \mathfrak{F}_1'$ — complex forces at the four-pole input,
$\mathfrak{F}_2, \mathfrak{F}_2'$ — complex forces at the four-pole output,
N — number of isolators,
c_L — propagation speed of longitudinal waves,
f — frequency,
f_0 — natural frequency of the one-mass-system (see Fig. 16),
f_1 — first natural continuum frequency of the isolators,
$\mathfrak{h}$ — complex admittance,
$|\mathfrak{h}|, h$ — modulus of admittance,

* In this article all complex quantities are expressed by Gothic letters.

h_D – floor admittance,
h_F – admittance of the test-foundation,
h_I – admittance of isolators,
h_M – machine admittance,
k – wave propagation number,
l – length of a longitudinally vibrating continuum,
m – mass,
n – continuum compliance; spring elasticity in the frequency range without natural continuum frequencies,
v – complex velocity,
$\tilde{v}$ – rms. value of velocity,
v_D – velocity at the place of machine mounting,
v_F – vertical velocity component at the test-foundation,
v_M – velocity of the machine,
v_1, v_1' – complex velocities at the four-pole input,
v_2, v_2' – complex velocities at the four-pole output,
η – loss factor,
λ – wave length,
ϱ – density,
$\omega = 2\pi f$ – angular frequency.

1. Introduction

Every longitudinally vibrating continuum has natural frequencies which depend on its elastic properties and its mass. With a constant cross-section the frequency f_ν, for example, at which acoustic waves are freely transmitted by a structure-borne sound isolator due to natural resonance can be computed from

$$f_\nu = \nu \cdot \frac{1}{2}\sqrt{\frac{1}{nm}} \qquad (\nu = 1, 2, 3, \ldots). \tag{1}$$

It is well-known that such natural continuum frequencies occur also in the rubber and steel springs which are used for structure-borne sound isolation. Therefore, it does not suffice to know the spring compliance when computing e.g. the structure-borne sound of buildings excited at high frequencies by machines with elastic supports. To be able to compute the vibration transmission or isolation when structure-borne sound isolators are coupled with the other vibrating structures (e.g. machine casing, supporting structure) one must know the frequency-dependent four-pole parameters of the continuum and include them in the computation.

In the following we should like to show how to measure the four-pole parameters of structure-borne sound isolators in the acoustic frequency range for real loads. In addition, the practical application of four-pole parameters of springs is explained when computing both the structure-borne sound isolation of a spring with a head mass, and the structure-borne sound excitation at the place of mounting of elastically supported machines.

2. Computation and measurement of the four-pole parameters of structure-borne sound isolators

2.1. Theoretical frequency response of the four-pole parameters of springs. We proceed from the wave equation for the velocity $v(x)$ of a longitudinal vibrating elastic continuum

$$AE\frac{\partial^2 v}{\partial x^2} - \varrho A\frac{\partial^2 v}{\partial t^2} = 0. \tag{2}$$

The connection between the force $F(x,t)$ and the velocity $v(x,t)$ is as follows

$$\frac{\partial F}{\partial t} = -AE\frac{\partial v}{\partial x}. \tag{3}$$

Solving (2) for the case of harmonic excitation, we get the general solution

$$v(x) - C_1\cos hjk(l-x) + C_2\sin hjk(l-x). \tag{4}$$

Considering the boundary conditions and notation according to Fig. 1 we obtain the following four-pole equations which connect the complex input quantities $\mathfrak{F}(0)$, $\mathfrak{v}(0)$ and the output quantities $\mathfrak{F}(l)$, $\mathfrak{v}(l)$:

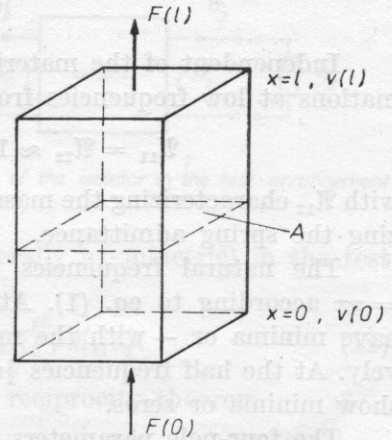

Fig. 1. Derivation of the four-pole parameters of a longitudinally vibrating continuum.

$$\begin{aligned}\mathfrak{F}(0) &= \cos hjkl\cdot\mathfrak{F}(l) + \frac{AEk}{\omega}\sin hjkl\cdot\mathfrak{v}(l),\\ \mathfrak{v}(0) &= \frac{\omega}{AEk}\sin hjkl\cdot\mathfrak{F}(l) + \cos hjkl\cdot\mathfrak{v}(l).\end{aligned} \tag{5}$$

We adopted the form of the four-pole equations with the coefficients $\mathfrak{A}_{ik}$ of the chain matrix which are used in references [2, 5, 6] and [7] and others

to characterize the vibration isolators:

$$\mathfrak{F}(0) = \mathfrak{A}_{11}\mathfrak{F}(l) + \mathfrak{A}_{12}\mathfrak{v}(l), \quad \mathfrak{v}(0) = \mathfrak{A}_{21}\mathfrak{F}(l) + \mathfrak{A}_{22}\mathfrak{v}(l). \tag{6}$$

According to [1] the material damping can be described approximately by a complex wave propagation number

$$\mathfrak{k} = \frac{\omega}{C_L}\left(1 - j\frac{\eta}{2}\right) = k_0\left(1 - j\frac{\eta}{2}\right). \tag{7}$$

The four-pole equations (5) now take the following form:

$$\begin{vmatrix} \mathfrak{F}(0) \\ \mathfrak{v}(0) \end{vmatrix} = \begin{vmatrix} \cos h\left(\frac{\eta}{2} + j\right) k_0 l & \frac{AE_0k_0}{\omega}\left(1 + j\frac{\eta}{2}\right)\sin h\left(\frac{\eta}{2} + j\right)k_0 l \\ \frac{\omega}{AE_0k_0}\left(1 - j\frac{\eta}{2}\right)\sin h\left(\frac{\eta}{2} + j\right)k_0 l & \cos h\left(\frac{\eta}{2} + j\right)k_0 l \end{vmatrix} \begin{vmatrix} \mathfrak{F}(l) \\ \mathfrak{v}(l) \end{vmatrix}. \tag{8}$$

When the damping is very small ($\eta \approx 0$) then the four-pole matrix becomes:

$$(A) = \begin{pmatrix} \cos k_0 l & j\omega m \frac{\sin k_0 l}{k_0 l} \\ j\omega n \frac{\sin k_0 l}{k_0 l} & \cos k_0 l \end{pmatrix}. \tag{9}$$

Independent of the material damping, one obtains the following approximations at low frequencies from equation (8):

$$\mathfrak{A}_{11} = \mathfrak{A}_{22} \approx 1, \quad \mathfrak{A}_{12} \approx j\omega m, \quad \mathfrak{A}_{21} \approx j\omega n, \tag{10}$$

with $\mathfrak{A}_{12}$ characterizing the mass impedance of the continuum and $\mathfrak{A}_{21}$ characterizing the spring admittance.

The natural frequencies of longitudinal vibrating continua are at $k_0 l = \nu\pi$ according to eq. (1). At these frequencies the parameters $\mathfrak{A}_{12}$ and $\mathfrak{A}_{21}$ have minima or – with the material damping disappearing – zeros, respectively. At the half frequencies $\frac{1}{2}\nu f_\nu$ (i.e. $k_0 l = \nu \cdot \pi/2$) the parameters $\mathfrak{A}_{11}$ and $\mathfrak{A}_{22}$ show minima or zeros.

The four-pole parameters were determined for springs with different material damping. The frequency characteristics are plotted in Fig. 6 to 12 for comparison with the measured results and discussed in section 2.4.

2.2. Fundamentals for the measurement of the four-pole parameters of springs. Several proposals for the measurement of the four-pole parameters of vibration isolators have already been described [6-9].

The disadvantage of these methods, however, is that the four-pole parameters of the springs cannot be determined under a real load. For example, the method described in [6, 8] requires two measurements (with the static

load of the spring ≈ 0 N or < 200 N). Thus it is not possible to carry out an exact determination of the load-dependent vibration characteristics, in particular, of rubber springs.

We therefore developed a measuring method permitting measurement of the four-pole parameters of vibration isolators at static loads which correspond to practical cases of isolators. These parameters will be different for different static loads applied in the experiment. This method is necessarily more complicated than the methods described in [6-9] and those used for determining the four-pole parameters of networks in electrical engineering, because the "no-load" case (i.e. when static load is equal to zero) will not be used in the measurements.

In the initial state of the four-pole which is to be measured, the following relations for the input and output quantities will be valid (see Fig. 2):

$$\mathfrak{F}_1 = \mathfrak{A}_{11}\mathfrak{F}_2 + \mathfrak{A}_{12}\mathfrak{v}_2, \quad \mathfrak{v}_1 = \mathfrak{A}_{21}\mathfrak{F}_2 + \mathfrak{A}_{22}\mathfrak{v}_2. \tag{11}$$

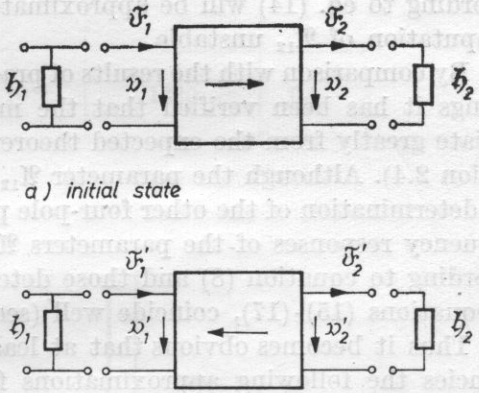

Fig. 2. Derivation of the measuring method for the determination of four-pole parameters of vibration isolators

After reversal of the isolator (which is generally asymmetric) in the test arrangement we obtain

$$\mathfrak{F}_1' = \mathfrak{A}_{22}\mathfrak{F}_2' + \mathfrak{A}_{12}\mathfrak{v}_2', \quad \mathfrak{v}_1' = \mathfrak{A}_{21}\mathfrak{F}_2' + \mathfrak{A}_{11}\mathfrak{v}_2'. \tag{12}$$

We took into consideration that due to the reciprocity theorem

$$\mathfrak{A}_{11}\mathfrak{A}_{22} - \mathfrak{A}_{12}\mathfrak{A}_{21} = 1. \tag{13}$$

The relationships for the determination of the chain matrix parameters follow from equations (11)-(13):

$$\mathfrak{A}_{12} = \frac{\dfrac{\mathfrak{F}_1'}{\mathfrak{F}_2'} - \dfrac{\mathfrak{F}_2}{\mathfrak{F}_1}}{\dfrac{\mathfrak{v}_1}{\mathfrak{F}_1} + \dfrac{\mathfrak{v}_2'}{\mathfrak{F}_2'}} \tag{14}$$

$$\mathfrak{A}_{22} = \frac{\mathfrak{F}_2}{\mathfrak{F}_1} + \frac{\mathfrak{v}_1}{\mathfrak{F}_1}\,\mathfrak{A}_{12}, \tag{15}$$

$$\mathfrak{A}_{11} = \frac{\mathfrak{F}_1}{\mathfrak{F}_2} - \frac{\mathfrak{v}_2}{\mathfrak{F}_2}\,\mathfrak{A}_{12}, \tag{16}$$

$$\mathfrak{A}_{21} = \frac{\mathfrak{v}_1}{\mathfrak{F}_2} - \frac{\mathfrak{v}_2}{\mathfrak{F}_2}\,\mathfrak{A}_{22}. \tag{17}$$

If a vibration isolator behaves approximately like an ideal spring in a given frequency range (i.e. no natural continuum frequencies occur), then the input and output forces are nearly equal: $\mathfrak{F}_1 \approx \mathfrak{F}_2$. In addition $\mathfrak{F}_1 = \mathfrak{F}_1'$ and $\mathfrak{F}_2 = \mathfrak{F}_2'$ is valid for symmetric isolators. Thus it follows that outside the natural continuum frequencies the numbers in the numerator of the expression for $\mathfrak{A}_{12}$ according to eq. (14) will be approximately equal, which makes the numerical computation of $\mathfrak{A}_{12}$ unstable.

By comparison with the results of practical investigations of steel and rubber springs it has been verified that the measured results of the parameter $\mathfrak{A}_{12}$ deviate greatly from the expected theoretical frequency characteristic (see also section 2.4). Although the parameter $\mathfrak{A}_{12}$ is included in equations (15)-(17) for the determination of the other four-pole parameters, it has been shown that the frequency responses of the parameters $\mathfrak{A}_{11}$, $\mathfrak{A}_{22}$ and $\mathfrak{A}_{21}$ which were computed according to equation (8) and those determined from measurements according to equations (15)-(17), coincide well (section 2.4).

Thus it becomes obvious that at least outside the natural continuum frequencies the following approximations for symmetrical springs are possible:

$$\mathfrak{A}_{11} = \frac{\mathfrak{F}_1}{\mathfrak{F}_2} = \mathfrak{A}_{22}, \tag{18}$$

$$\mathfrak{A}_{21} = \frac{\mathfrak{v}_1}{\mathfrak{F}_2} - \frac{\mathfrak{v}_2}{\mathfrak{F}_2}\,\frac{\mathfrak{F}_1}{\mathfrak{F}_2}. \tag{19}$$

The justification of relationships (18) and (19) is discussed in section 2.4.

2.3. Measurement of the four-pole parameters of different springs. The test objects for the measurement of the four-pole parameters are summarised in Table 1.

Figures 3 and 4 show the test arrangement. An electrodynamic exciter serves as a vibration source. The static load was measured with the help of a KWH 200 type semiconducting force transducer (manufacturer: VEB Robotron Messelektronik Dresden). To measure the exciting forces and velocities according to Fig. 3, we used quartz load-cells and piezoelectric pick-ups. The mechanical measuring chain was installed in a sectional steel frame so as to apply any static load up to 1 kN with the help of a regulating screw.

Table 1. Test objects for the determination of the four-pole parameters

Spring type	Mass [kg]	Compliance [$s^2 \cdot kg^{-1}$]	First natural continuum frequency computed from eq. (1) [Hz]	Loss factor
Steel spring (No. 25 spring from P50/125 Type Vibration Isolator of VEB Schwingungsisolatorenbau Radebeul)	0.08	$7.1 \cdot 10^{-5}$	210	10^{-4}
Prismatic rubber spring ($27 \times 27 \times 63$ mm^3)	0.560	$3 \cdot 10^{-6}$	1220	0.1

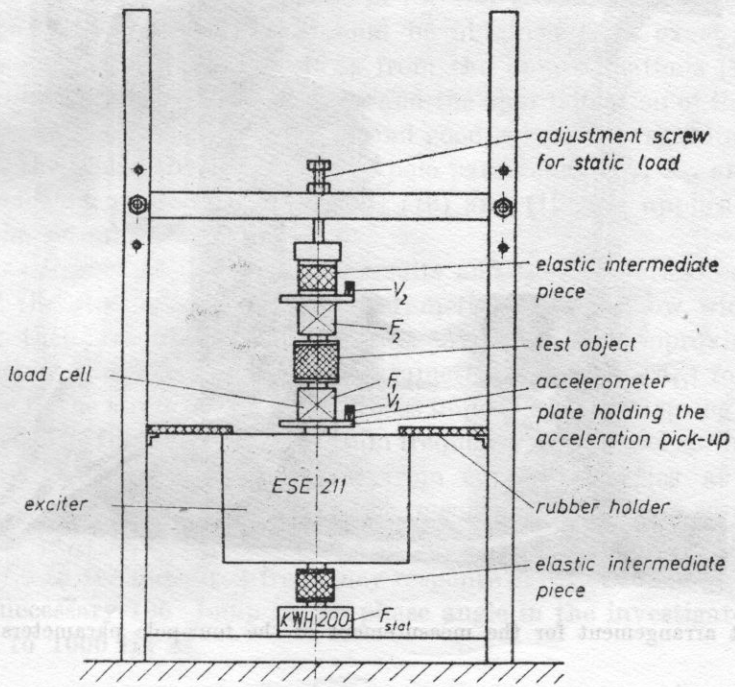

Fig. 3. Test arrangement for the determination of the four-pole parameters of vibration isolators

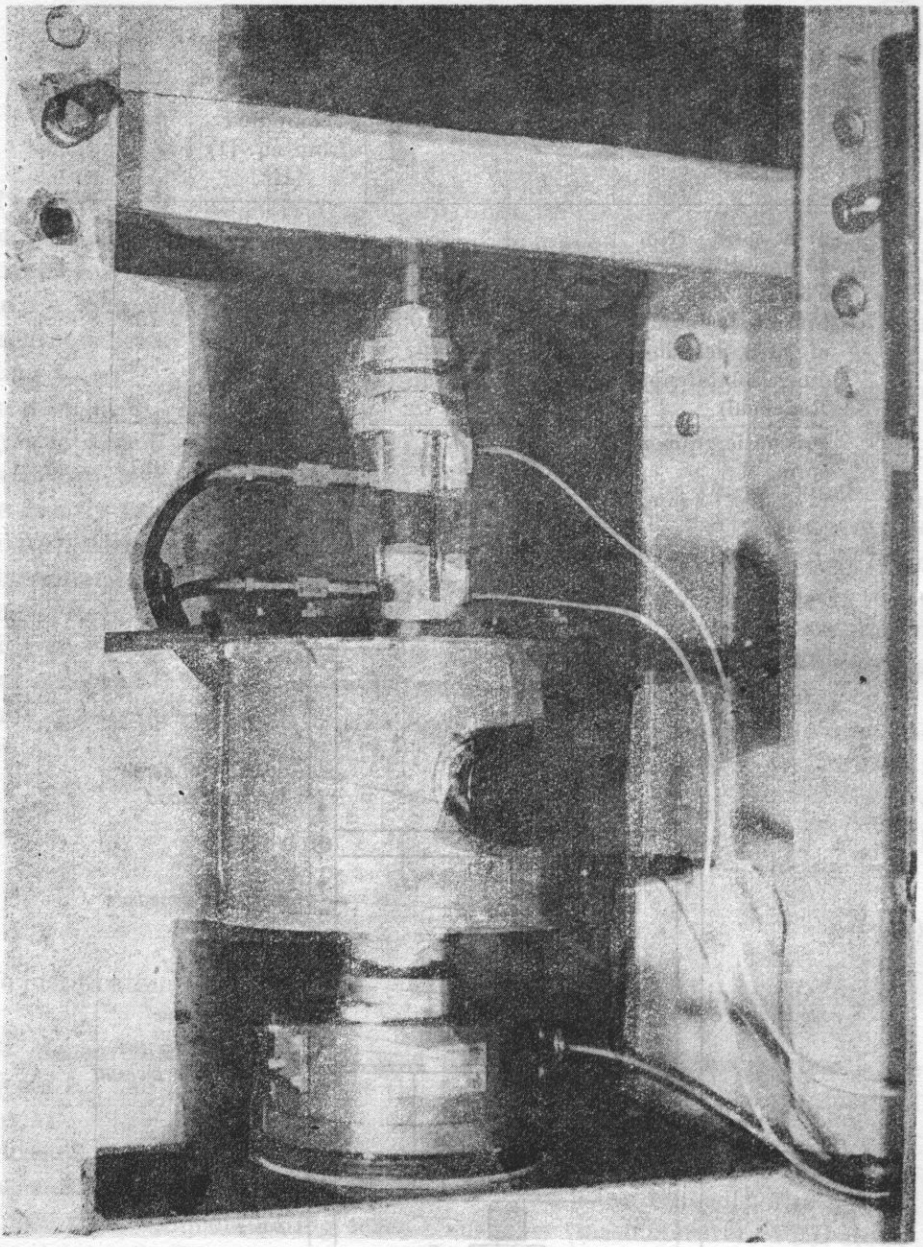

Fig. 4. Test arrangement for the measurement of the four-pole parameters of springs

It must be mentioned that it was not possible to measure the forces immediately at the boundary surfaces of the investigated springs, because additional masses (such as pressure plates, vibration pick-ups) were brought in between the electromechanical transducers of the load-cells and the test object. Considering Fig. 5 the measured forces F_{1m} and F_{2m} were corrected by in-phase substraction and addition of the mass forces. The measurement of the phase — angles was made by use of an RFT phase-detector.

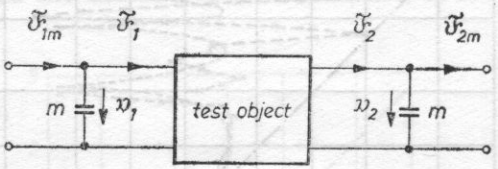

Fig. 5. Correction of the measured forces in the determination of the four-pole parameters of vibration isolators

$$\mathfrak{F}_1 = \mathfrak{F}_{1m} - j\omega v_1 m$$

$$\mathfrak{F}_2 = \mathfrak{F}_{2m} + j\omega v_2 m$$

2.4. Comparison of the four-pole parameters of different spring types determined in the experiments and with those found by computation. Figures 6 to 8 show the comparison between the four-pole parameters of the steel spring which were computed according to equation (9) and those obtained from measurement. The measurement results could be obtained from exact relationships in equations (14) to (17) as well as from the approximations (18) and (19). When comparing the exact calculation and the approximation of the parameters determined by the measurements, we find good agreement regarding the moduli as well as the phase angles of the four-pole parameters $\mathfrak{A}_{11}$, $\mathfrak{A}_{22}$ and $\mathfrak{A}_{21}$. Thus, it has been shown that approximations (18) and (19) are applicable not only outside the resonance frequencies.

The experimental measurement results and the theoretical computational results of the steel spring four-pole parameters do not show wide deviations regarding their essential characteristics. According to approximations (10) the frequency characteristics of the parameters $|\mathfrak{A}_{12}|$ and $|\mathfrak{A}_{21}|$ for $f < 100$ Hz come close to the straight lines of the mass impedance of the spring or the spring admittance. The first natural continuum frequency of the steel spring ($m = 80$ g, $n = 7.1 \cdot 10^{-5}\ \mathrm{s^2 \cdot kg^{-1}}$) as determined from equation (1) lies at $f_1 = 210$Hz. The first and second minimum of the measured frequency response of the parameters $|\mathfrak{A}_{11}|$ and $|\mathfrak{A}_{22}|$ lie — as can be expected from equation (9) — at $\frac{1}{2}f_1$ and $\frac{3}{2}f_1$. In the measured frequency response of $|\mathfrak{A}_{21}|$ evident minima appear with the necessary 180° jump in the phase angle in the investigated frequency range up to 1000 Hz at

$$f = \frac{\nu}{2}\sqrt{\frac{1}{mn}} \qquad (\nu = 1, 2, 3).$$

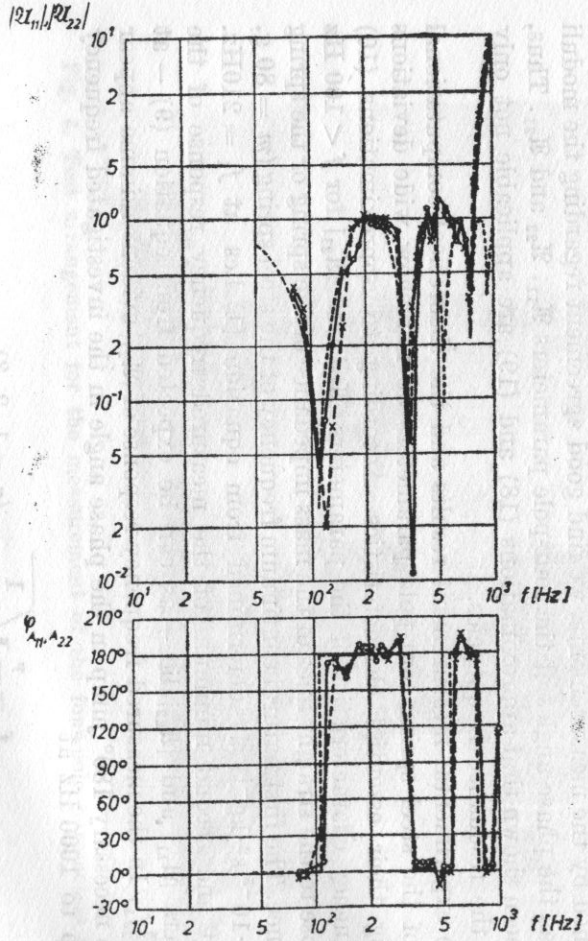

Fig. 6. Four-pole parameters $\mathfrak{A}_{11}$ and $\mathfrak{A}_{22}$ of a No. 25 steel spring

– – – theoretical curve using eq. (9), ×– – –× computed from measured data using eq. (16), ○——○ approximation using eq. (18)

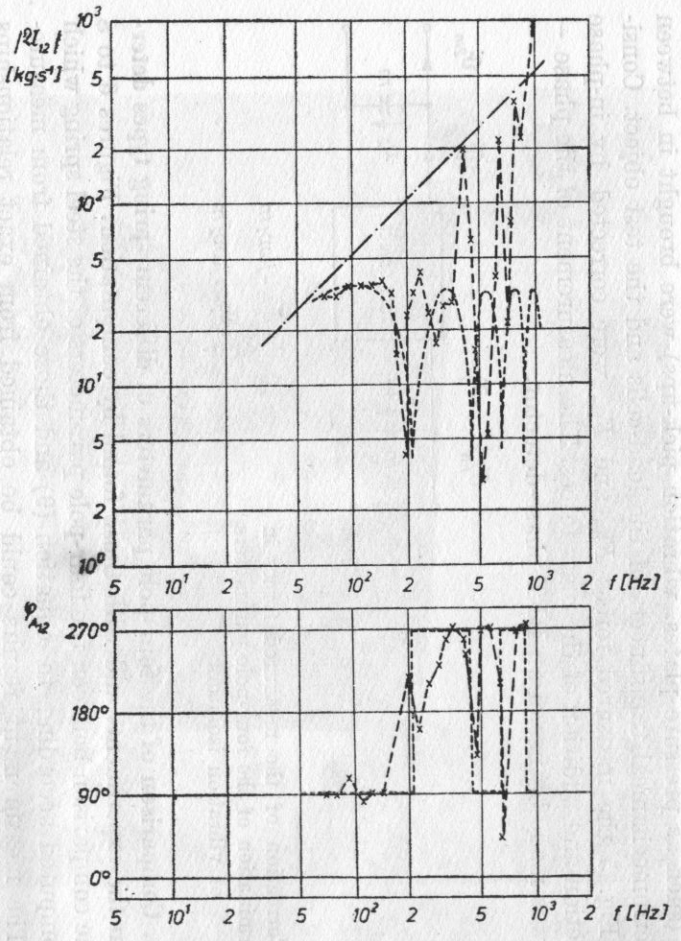

Fig. 7. Four-pole parameter $\mathfrak{A}_{12}$ of a No. 25 steel spring

– – – theoretical curve using eq. (9), ×– – –× computed from measured data using eq. (14), –·– mass impedance of the spring mass (m = 80 g)

To interpret the increase of maxima in the frequency response of $|\mathfrak{A}_{21}|$ we computed the theoretical response for different loss factors according to equation (8). The results were plotted in Fig. 9 to be compared with the measured frequency response of $|\mathfrak{A}_{21}|$. One finds that the increase in maxima of $|\mathfrak{A}_{21}|$ can be explained by a higher loss factor. At the same time the question is left open as to why there are still evident minima between the increasing maxima in the curve determined from measured results which do not appear in the theoretical results. Probably a damping law is concerned, which is unknown as yet, and which should be considered in the theoretical determination of the four-pole parameters of steel springs.

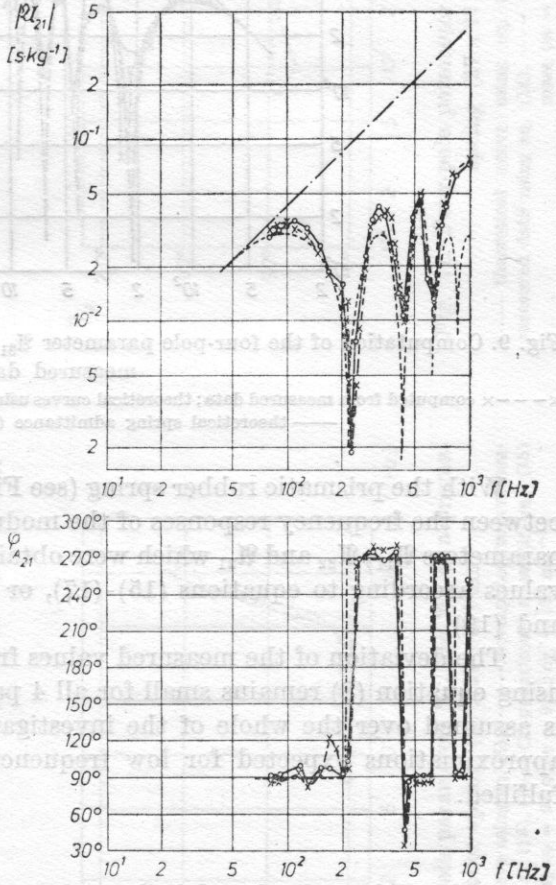

Fig. 8. Four-pole parameter $\mathfrak{A}_{21}$ of a No. 25 steel spring
– – – theoretical curve using eq. (9), ×– – –× computed from measured data using eq. (17), O——O approximation using eq. (19), –·– theoretical spring admittance ($n = 7.1 \cdot 10^{-5}$ s^2·kg^{-1})

The parameter $|\mathfrak{A}_{12}|$ in which one expects the same frequency response as in $|\mathfrak{A}_{21}|$ according to equation (9) shows only allusively a regularity in the position of the minima. The reason for this difference between the computed and the measured values lies in the difficulties occurring in the determination of $|\mathfrak{A}_{12}|$ from the measured values as has been mentioned already in section 2.2.

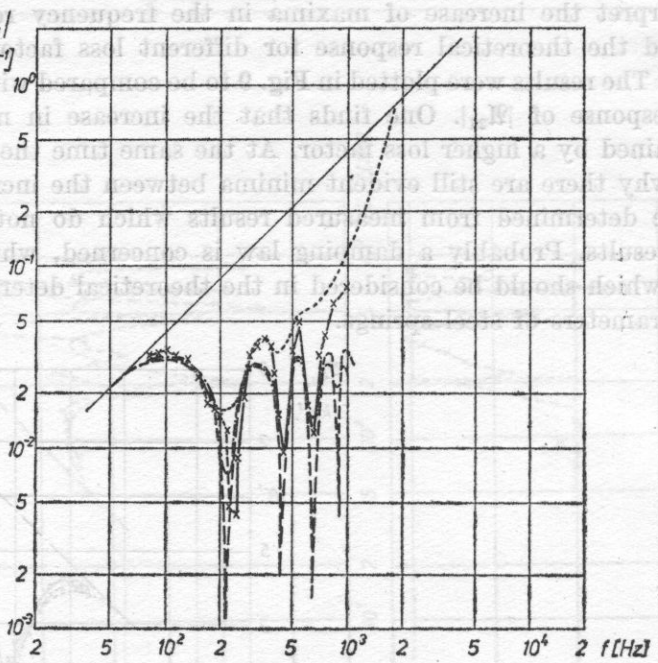

Fig. 9. Computation of the four-pole parameter $\mathfrak{A}_{21}$ of a No. 25 steel spring from theory and measured data

×– – –× computed from measured data; theoretical curves using eq. (8), – – – $\eta = 0.01$, –·– $\eta = 0.1$, ------ $\eta = 0.3$, —— theoretical spring admittance ($n = 7.1 \cdot 10^{-5}$ s^2·kg^{-1})

With the prismatic rubber spring (see Fig. 10 to 12) there is good agreement between the frequency responses of the moduli and phase angles of the four-pole parameters $\mathfrak{A}_{11}$, $\mathfrak{A}_{22}$ and $\mathfrak{A}_{21}$ which were obtained both exactly from the measured values according to equations (15)-(17), or approximately from equations (18) and (19).

The deviation of the measured values from the theoretical values computed using equation (8) remains small for all 4 parameters if a loss factor of $\eta = 0.1$ is assumed over the whole of the investigated frequency range. Obviously, the approximations expected for low frequencies according to equation (10) are fulfilled.

3. Examples of the application of the four-pole parameters of structure-borne sound isolators

3.1. Computation of the structure-borne sound isolation of a longitudinally vibrating continuum with an attached head mass. As a measure of the structure-borne sound isolation the ratio of the velocities v_1 and v_2 at the input or output of a vibration isolator which is installed in a spring — mass — system (see Fig. 13) will be considered. This velocity ratio characterizes the effect of a struc-

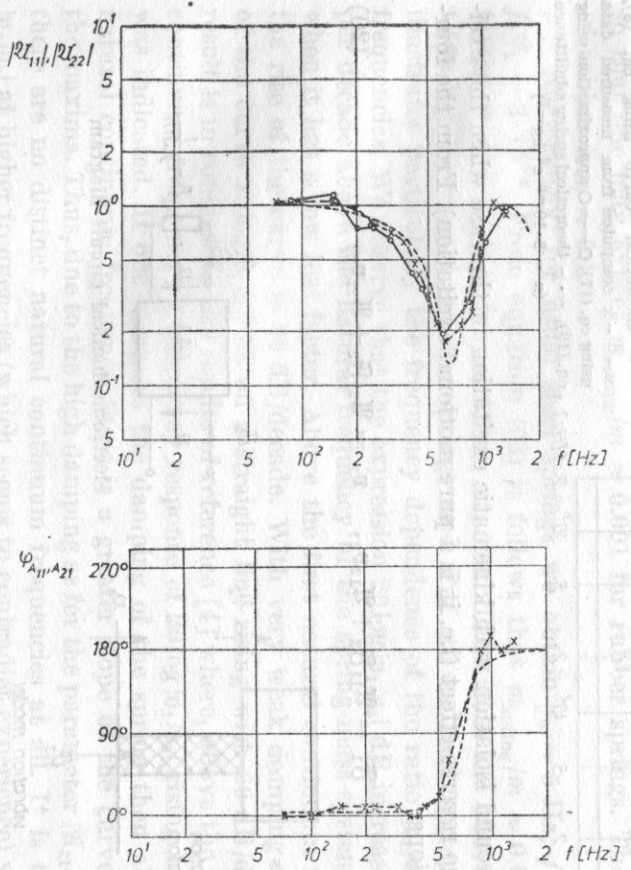

Fig. 10. Four-pole parameters $\mathfrak{A}_{11}$ and $\mathfrak{A}_{22}$ of a prismatic rubber spring $(27 \times 27 \times 63)$ mm³

------ theoretical curve using eq. (8), ×– – –× computed from measured data using eq. (16), O——O approximation using eq. (18) (l = 6.3 cm; m = 56 g; η = 0.1; c_L = 165 ms^{-1})

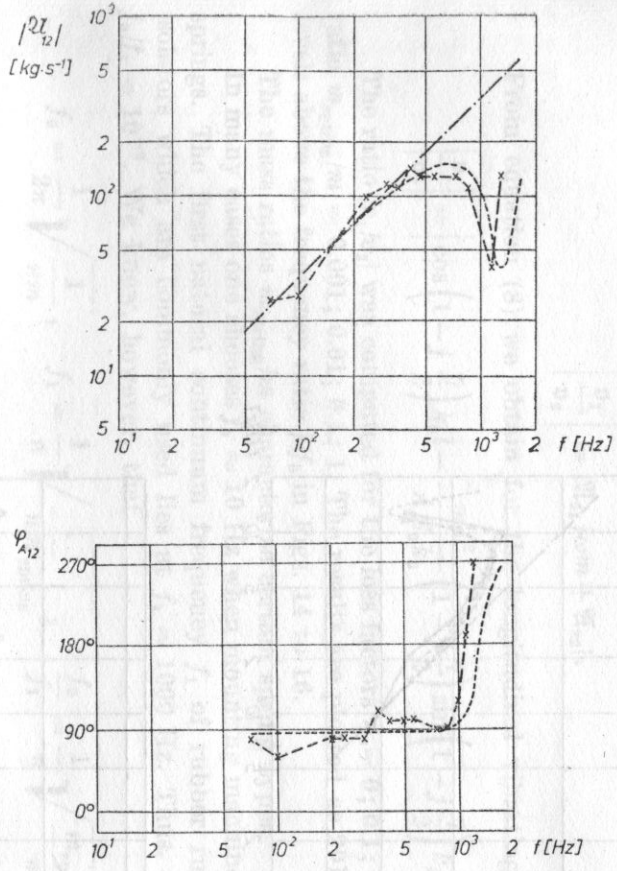

Fig. 11. Four-pole parameter $\mathfrak{A}_{12}$ of a prismatic rubber spring $(27 \times 27 \times 63)$ mm³

------ theoretical curve using eq. (8), ×– – –× computed from measured data using eq. (14), –·– mass impedance of the spring mass (m = 56 g)

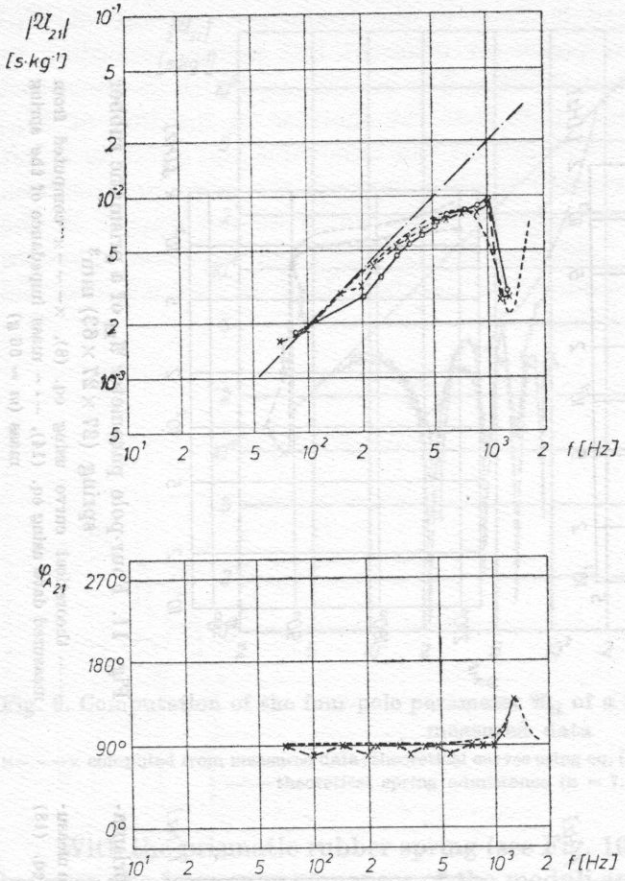

Fig. 12. Four-pole parameter $\mathfrak{A}_{21}$ of a prismatic rubber spring

------ theoretical curve using eq. (8), ×– – –× computed from measured data using eq. (17), O——O approximation using eq. (19), – · – theoretical spring admittance ($n = 3 \cdot 10^{-6}$ s^2·kg^{-1})

ture-borne sound isolation with kinematic excitation in the case when the excitation has no reverse effect (i.e. it is a pure motional excitation). From the four-pole equations

$$\mathfrak{F}_1 = \mathfrak{A}_{11}\mathfrak{F}_2 + \mathfrak{A}_{12}\mathfrak{v}_2, \qquad \mathfrak{v}_1 = \mathfrak{A}_{21}\mathfrak{F}_2 + \mathfrak{A}_{22}\mathfrak{v}_2, \tag{20}$$

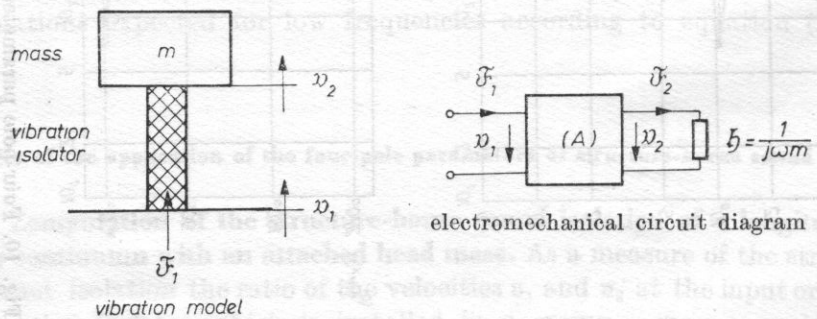

Fig. 13. Characterization of the structure-borne sound damping of vibration isolators

and the condition $\mathfrak{F}_2 = j\omega m \mathfrak{v}_2$ to be read from the circuit diagram (see. Fig. 13) one obtains as the modulus of the velocity ratio:

$$\left|\frac{\mathfrak{v}_1}{\mathfrak{v}_2}\right| = |\mathfrak{A}_{21} j\omega m + \mathfrak{A}_{22}|. \tag{21}$$

From equation (8) we obtain for the longitudinal vibrating continuum

$$\left|\frac{\mathfrak{v}_1}{\mathfrak{v}_2}\right| = \left|\cos\left(1-j\frac{\eta}{2}\right)k_0 l - \frac{m\omega^2}{AE_0 k_0}\left(1-j\frac{\eta}{2}\right)\sin\left(1-j\frac{\eta}{2}\right)k_0 l\right|. \tag{22}$$

The ratio $|\mathfrak{v}_1/\mathfrak{v}_2|$ was computed for the loss factors $\eta = 0;\ 0.1;\ 0.3$ with the ratio $m_{\text{spring}}/m = 0.001;\ 0.01;\ 0.1;\ 1$. The results are plotted as $20\log|\mathfrak{v}_1/\mathfrak{v}_2|$ dB levels above the frequency ratio f/f_0 in Figs. 14 to 16.

The mass ratios m_{spring}/m characterize certain spring types.

In many cases one chooses $f_0 \approx 10$ Hz when mounting machines on rubber springs. The first natural continuum frequency f_1 of rubber rubber spring isolators which are commonly used lies at $f_1 \approx 1000$ Hz. Thus, one obtains $f_0/f_1 = 10^{-2}$. We know, however, that

$$f_0 = \frac{1}{2\pi}\sqrt{\frac{1}{nm}}, \quad f_1 = \frac{1}{\pi}\sqrt{\frac{1}{nm_{\text{spring}}}}, \quad \frac{f_0}{f_1} = \frac{1}{\pi}\sqrt{\frac{m_{\text{spring}}}{m}},$$
$$\frac{m_{\text{spring}}}{m} \approx 10\cdot\left(\frac{f_0}{f_1}\right)^2, \tag{23}$$

so that one may expect $m_{\text{spring}}/m \approx 0.001$ for rubber springs. The loss factor of rubber is $\eta \approx 0.1$.

Analogously, for usual steel springs we obtain $f_0 \approx 5$ Hz, $f_1 \approx 150$ Hz, $f_0/f_1 = 3\cdot 10^{-2}$. From equation (23) it follows that $m_{\text{spring}}/m \approx 0.01$. The loss factor of steel springs is $\eta \approx 0.001, \ldots, 0.01$. Thus from the above considerations Fig. 14 refers to rubber springs and Fig. 15 to steel springs. Fig. 16 illustrates particularly the frequency dependence of the ratio $|\mathfrak{v}_1/\mathfrak{v}_2|$ at higher frequencies. We observe that the expression $20\log|\mathfrak{v}_1/\mathfrak{v}_2|$ dB increases by 40 dB per decade above the natural frequency of the spring-mass-system considered when it has a low loss factor. Above the first natural continuum frequency f_1 the rise of the curve is 80 dB/decade. With very weak damping the maxima of the curve $20\log|\mathfrak{v}_1/\mathfrak{v}_2|$ lie on a straight line rising with 20 dB/decade. This result is in contrast to the results of reference [4] where, above the first natural continuum frequency, a frequency response of $20\log|\mathfrak{v}_1/\mathfrak{v}_2|$ rising by 80/decade was indicated. If one increases the damping of the spring then above second natural continuum frequency there is a greater slope of the curve connecting the maxima. Thus, due to the high damping as for the parameter $|\mathfrak{A}_{21}|$ in Fig. 9 — there are no distinct natural continuum frequencies at all. It is this slope of $|\mathfrak{v}_1/\mathfrak{v}_2|$ at higher frequencies (which seems to contradict experience) which causes us to be interested in the following question: Can a strongly damped steel

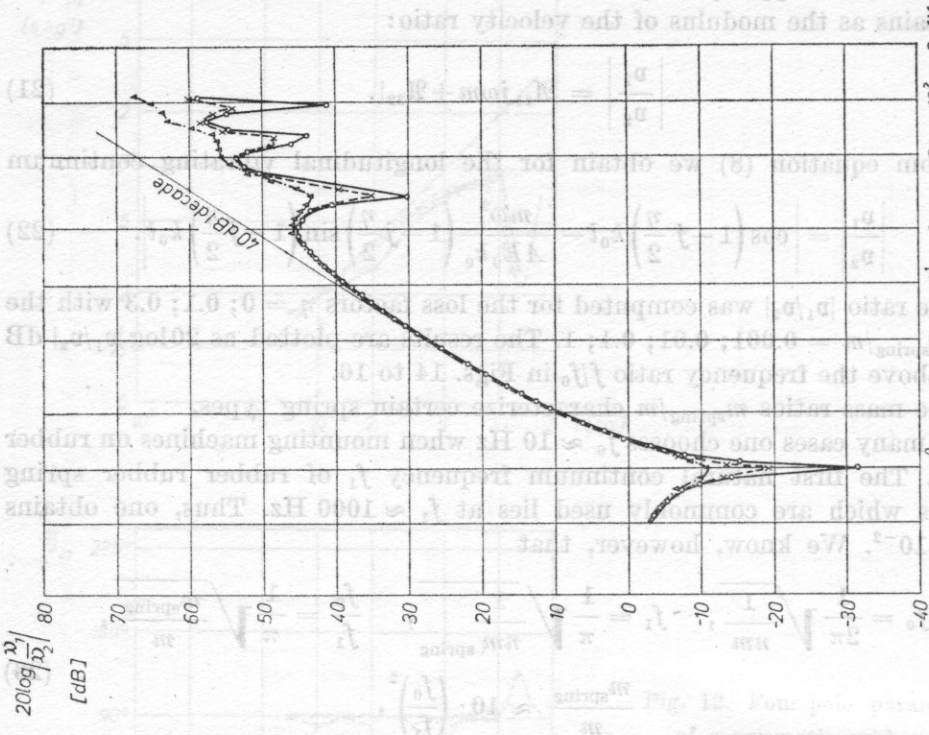

Fig. 15. Velocity ratio level $|v_1/v_2|$ for $m_{spring}/m = 0.01$
○——○ $\eta = 0$, × – – – × $\eta = 0.1$, △–·–△ $\eta = 0.3$

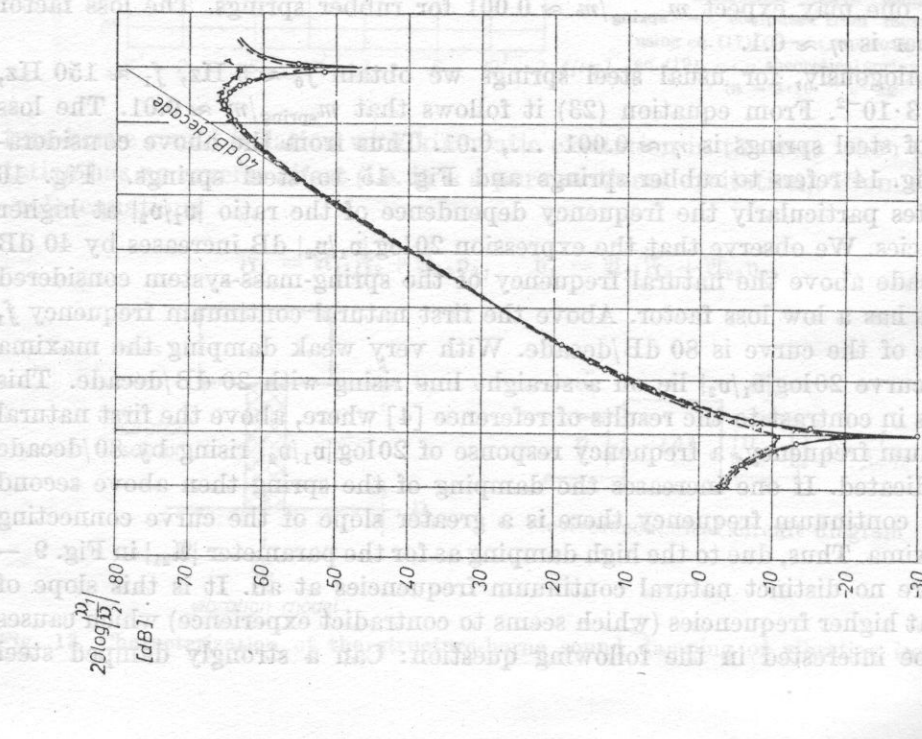

Fig. 14. Velocity ratio level $|v_1/v_2|$ for $m_{spring}/m = 0.001$
○——○ $\eta = 0$, × – – – × $\eta = 0.1$, △–·–△ $\eta = 0.3$

spring be more appropriate for structure-borne sound isolation than a rubber spring? Considering the available results this can be the case only if the $20\log|v_1/v_2|$ curve of the strongly damped steel spring will, due to its steeper

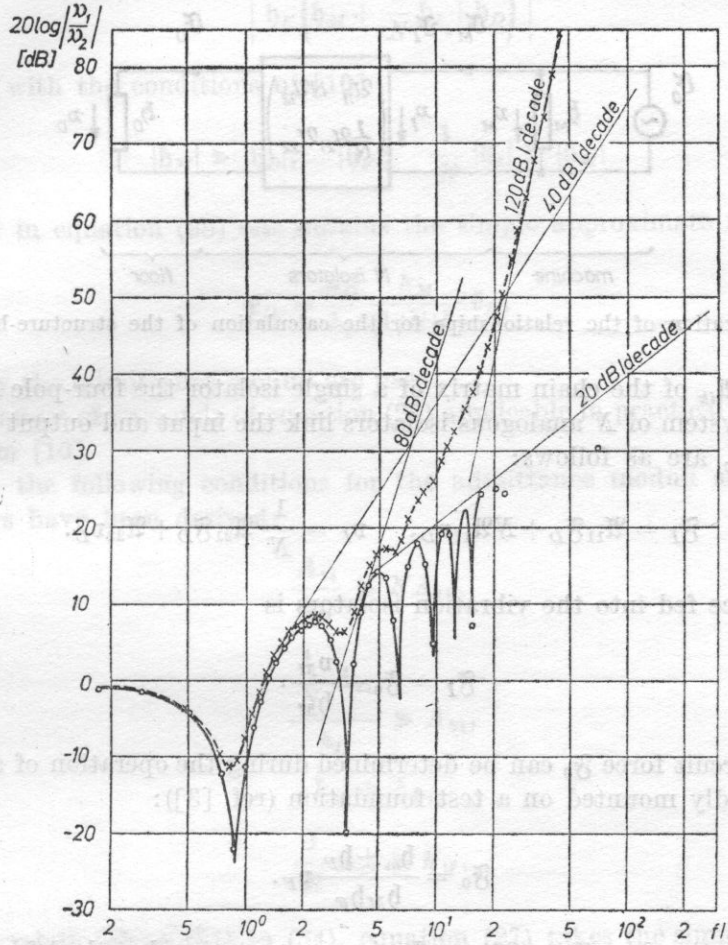

Fig. 16. Velocity ratio level $|v_1/v_2|$ for $m_{spring}/m = 1$
○——○ $\eta = 0$, ×– – –× $\eta = 0.3$

slope, intersect the curve of the rubber spring rising by 40 dB/decade above the second natural continuum frequency.

It can be seen from Fig. 15 that this circumstance will arise in the frequency range of interest (i.e. up to 1000 Hz) only if the steel spring isolators will have a loss factor $\eta \geqslant 0.3$ and if $m_{spring}/m \to 1$. This is realizable only by "series--connected lumped-parameter systems" containing additive damping elements or otherwise damped springs.

3.2. Computation of the structure-borne sound excitation at the place of mounting of elastically supported machines. The general case of machine mounting on isolators with natural continuum frequencies can be characterized by the electromechanical circuit diagram shown in Fig. 17. Including the complex

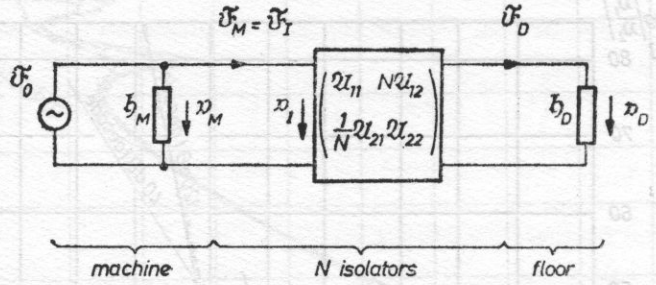

Fig. 17. Derivation of the relationships for the calculation of the structure-borne sound

coefficients $\mathfrak{A}_{ik}$ of the chain matrix of a single isolator the four-pole equations, which in a system of N analogous isolators link the input and output quantities (see Fig. 17), are as follows:

$$\mathfrak{F}_I = \mathfrak{A}_{11}\mathfrak{F}_D + N\mathfrak{A}_{12}\mathfrak{v}_D, \qquad \mathfrak{v}_I = \frac{1}{N}\mathfrak{A}_{21}\mathfrak{F}_D + \mathfrak{A}_{22}\mathfrak{v}_D. \tag{24}$$

The force fed into the vibration isolators is

$$\mathfrak{F}_I = \mathfrak{F}_0 - \frac{\mathfrak{v}_M}{\mathfrak{h}_M}. \tag{25}$$

The short-circuit force $\mathfrak{F}_0$ can be determined during the operation of a machine which is rigidly mounted on a test foundation (ref. [3]):

$$\mathfrak{F}_0 = \frac{\mathfrak{h}_m + \mathfrak{h}_F}{\mathfrak{h}_M \mathfrak{h}_F}\mathfrak{v}_F. \tag{26}$$

From relationships (24) - (26) we obtain a computational method for (multiplication) determining the rms. value of the velocity $\tilde{v}_D$ at the place of mounting of an elastically supported machine when the effective velocity $\tilde{v}_F$ (which is produced by the machine rigidly mounted on a test foundation) is known

$$\tilde{v}_D = \left| \frac{\mathfrak{h}_F + \mathfrak{h}_M}{\mathfrak{h}_F \mathfrak{h}_M \left[\left(\frac{\mathfrak{A}_{11}}{\mathfrak{h}_D} + N\mathfrak{A}_{12} \right) + \frac{1}{\mathfrak{h}_M} \left(\frac{1}{N}\frac{\mathfrak{A}_{21}}{\mathfrak{h}_D} + \mathfrak{A}_{22} \right) \right]} \right| \tilde{v}_F. \tag{27}$$

Assuming that the natural continuum frequency of the applied isolators does not lie within the frequency range up to 1000 Hz which is of interest, we can introduce the four-pole parameters of an ideal spring according to equation

(10) into eq. (27). It then becomes

$$\tilde{v}_D = \left| \frac{\mathfrak{h}_D(\mathfrak{h}_F + \mathfrak{h}_M)}{\mathfrak{h}_F\left(\mathfrak{h}_M + \frac{1}{N}\mathfrak{h}_I + \mathfrak{h}_D\right)} \right| \tilde{v}_F. \tag{28}$$

Now, with the conditions of [10]

$$|\mathfrak{h}_M| \gg |\mathfrak{h}_D|, \quad |\mathfrak{h}_F|; \quad \frac{1}{N}|\mathfrak{h}_I| \gg |\mathfrak{h}_M| \tag{29}$$

considered in equation (28) one obtains the simple approximate relationship:

$$\tilde{v}_D = \frac{h_D}{h_F}\frac{h_M}{(1/N)h_I}\tilde{v}_F, \tag{30}$$

where only the admittance moduli are used.

The ranges of operands of equation (27) applicable in practical cases can be taken from [10].

Thus, the following conditions for the admittance moduli and four-pole parameters have been derived:

$$\frac{A_{11}}{h_D} \gg NA_{12}, \tag{31}$$

$$\frac{\frac{1}{N}A_{21}}{h_D} \gg A_{22}, \tag{32}$$

$$h_M \gg h_F, \tag{33}$$

$$\frac{1}{N}A_{21} \gg h_M. \tag{34}$$

With relationships (31) to (34), equation (27) takes the simple form

$$\tilde{v}_D = \frac{h_D h_M}{h_F \frac{1}{N}A_{21}}\tilde{v}_F. \tag{35}$$

Here, $\mathfrak{A}_{21}$ proves to be the most important parameter for the computation of the structure-borne sound excitation. The four-pole parameter $|\mathfrak{A}_{21}|$ rather than the isolator admittance h_I is set in eq. (35) which makes a difference to equation (30).

Fig. 18 shows the comparison of the results computed from equations (27), (28), (30) and (35) with the measured results relating to the mounting of a machine model on No. 25 steel springs (electrodynamic exciter on steel

mass, see ref. [10]). For a quantity characterizing the difference between computation and measurement we used the level difference ΔL_v between the computed and the measured velocity level at the place of mounting:

$$\Delta L_v = 20 \log \frac{\tilde{v}_{D\,\mathrm{comp.}}}{\tilde{v}_{D\,\mathrm{measur.}}} \quad [\mathrm{dB}]. \tag{36}$$

One can see that by using the isolator admittance in equations (28) and (30) there is considerable deviation between computation and measurement at $f > 100$ Hz. However, the application of the four-pole parameters from equation (27) or the parameter A_{21} from equation (35) characterizes the effect of the natural continuum frequencies of the steel springs much better. The results of Fig. 8 can be used to show this. The modulus of the four-pole parameter $\mathfrak{A}_{21}$ for $f > 100$ Hz clearly remains below the theoretical admittance of the No. 25 steel spring. This means that the springs used seem to be considerably harder due to the natural continuum frequencies than is indicated by the spring constant. The increasing difference between $|\mathfrak{h}_I|$ and $|\mathfrak{A}_{21}|$ in Fig. 8 corresponds to the difference between the measurement and the computation according to equations (28) and (30) which increases with frequency (see Fig. 18).

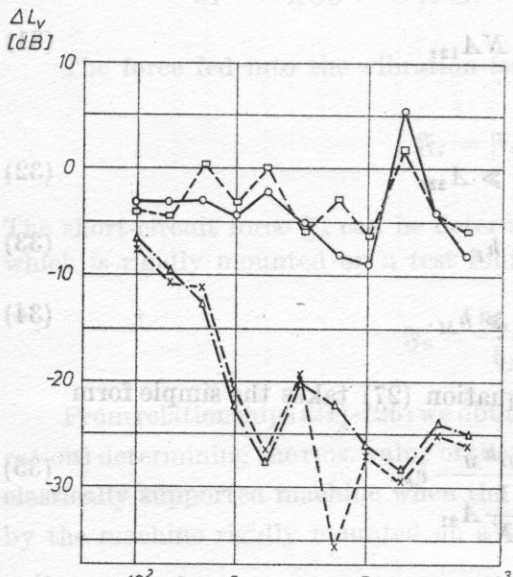

Fig. 18. Differences between the computed and measured velocity levels for the elastic mounting of a machine model on steel springs

○——○ computation with four-pole parameters using eq. (27), ×– – –× complex computation using eq. (28), △–·–△ approximation with h_I using eq. (35), □– – –□ approximation with $\mathfrak{A}_{21}$ using eq. (35)

The fact that the structure-borne sound excitation can be much better calculated by substituting A_{21} for h_I in equation (30) leads us to the conclusion that the compliance n of steel spring can be corrected above the first natural continuum frequency. Evidently, $h_I \approx A_{21}$, and with $h_I = \omega n$ for the steel

spring compliance (see eq. (9)) it follows that

$$n = \frac{1}{\omega} A_{21} \approx n_0 \frac{\sin k_0 l}{k_0 l} \tag{37}$$

(n_0 = steel spring compliance below the first natural continuum frequency).

On average, the compliance decreases with frequency and has additional minima at the natural continuum frequencies.

Experiments have shown that with rubber springs, due to the smaller influence of the natural continuum frequencies in the frequency range up to 1000 Hz, one can compute the structure-borne excitation from equation (30) and dispense with the four-pole parameters.

References

[1] L. Cremer, M. Heckl, *Körperschall*, Springer Verlag, Berlin – Heidelberg – New York 1967.

[2] J. J. Kljukin, *O kriterijach wibroizoljacii i sootnoszenijach mieżdu nimi*, Akusticzeskij Żurnał, **5**, 747-750 (1975).

[3] R. Melzig-Thiel, G. Meltzer, *Voraussetzungen und Ergebnisse bei der Berechnung der Körperschall-anregung von Gebäuden durch Maschinen*, Maschinenbautechnik **26**, 7, 306-310 (1977); **26**, 8, 371-374 (1977).

[4] E. Müller, G. Thien, G. Deutschbein, *Körperschalldämmung – Arbeitsfort-schrittsbericht, Referat auf der Informationstagung der FVV in Graz am 24.10.74*, Frankfurt/Main: Eigenverlag Daimler-Benz AG 1974, Schriftenreihe des Hrsg., Heft R 260.

[5] J. S. Snowdon, *Mechanical four-pole parameters and their application*, Journal of Sound and Vibration, **15**, 3, 307-324 (1971).

[6] J. Stenička, *Complex acoustical parameters of vibrating transmission through rubber insulators and their applications in experimental research*, Sammelband der 2. Nationalen Konferenz für Akustik, Varna 1975, Vortrag No. 3.

[7] P. Urban, *Theorie a metody mereni prenosu vibraci mechanickymi dily*, Studie CSAV, Praha; Academia 1973.

[8] P. Urban, *Untersuchungsmethoden der Schallausbreitung*, Proc. 7th ICA Congress, Budapest 1972, 19 N 7.

[9] J. Veit, *Bestimmung der Schallübertragungsdämpfung von Kompensatoren durch Messung ihrer Vierpolparameter Tagungsberichte, Der 5.* Tagung der Deutschen Arbeitsgemeinschaft für Akustik, DAGA 76 Heidelberg: o.V. 1976, 675-678.

[10] R. Melzig-Thiel, *Beiträge zur theoretischen und experimentallen Begründung eines Verfahrens für die Berechnung, Der Körperschallanregung von Gebäuden durch Maschinen*, Diss. A, Technische Universität Dresden, 1979.

Received on May 28, 1979; revised version on May 6, 1980.